

# Ultrafast Vibrational Spectroscopic Studies on the Photoionization of the $\alpha$ -Tocopherol Analogue Trolox C

*Anthony W. Parker<sup>1</sup>, Roger H. Bisby\*<sup>2</sup>, Gregory M. Greetham<sup>1</sup>, Philipp Kukura<sup>3</sup>, Kathrin M.  
Scherer<sup>1, 2</sup> and Michael Towrie<sup>1</sup>*

<sup>1</sup> Central Laser Facility, Research Complex at Harwell, STFC Rutherford Appleton Laboratory,  
Harwell Oxford, Didcot, Oxfordshire, OX11 0QX, UK

<sup>2</sup> Biomedical Science Research Institute, University of Salford, Salford M5 4WT, UK

<sup>3</sup> Department of Chemistry, University of Oxford, Oxford OX1 3QZ, UK

\*Corresponding author. Email [r.h.bisby@salford.ac.uk](mailto:r.h.bisby@salford.ac.uk), telephone +44(0)1614764773

## ABSTRACT

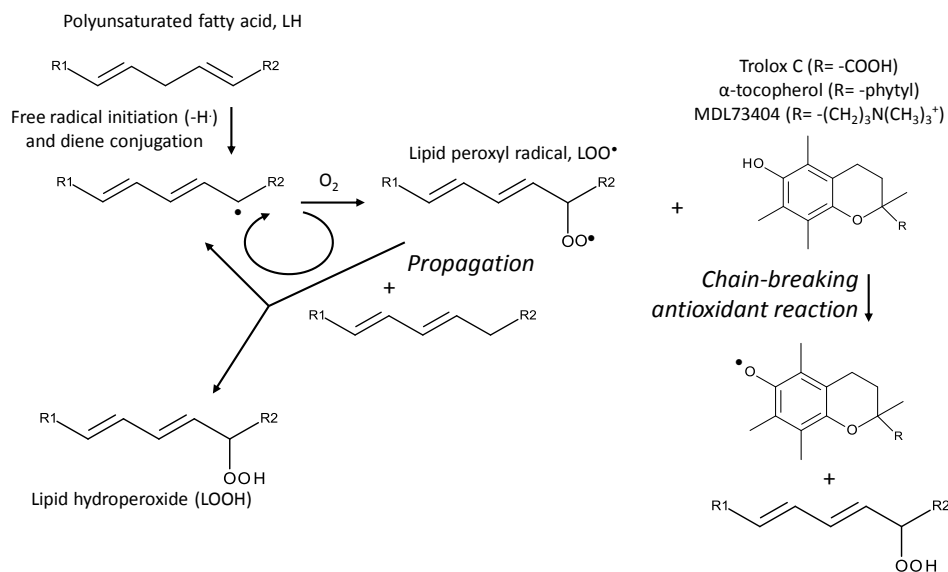
The initial events after photoexcitation and photoionization of  $\alpha$ -tocopherol (vitamin E) and the analogue Trolox C have been studied by femtosecond stimulated Raman spectroscopy, transient absorption spectroscopy and time-resolved infrared spectroscopy. Using these techniques it was possible to follow the formation and decay of the excited state, neutral and radical cation radicals and the hydrated electron that are produced under the various conditions examined.  $\alpha$ -Tocopherol and Trolox C in methanol solution appear to undergo efficient homolytic dissociation of the phenolic –OH bond to directly produce the tocopheroxyl radical. In contrast, Trolox C photochemistry in neutral aqueous solutions involves intermediate formation of a radical cation and the hydrated electron which undergo geminate recombination within 100 ps in competition with deprotonation of the radical cation. The results are discussed in relation to recently proposed mechanisms for the reaction of  $\alpha$ -tocopherol with peroxy radicals, which represents the best understood biological activity of this vitamin.

Keywords: Vitamin E,  $\alpha$ -tocopherol, Trolox C, ultrafast, stimulated Raman, time-resolved, infrared, photoionization

## INTRODUCTION

Antioxidants play a crucial role in biological systems, preventing oxidative stress that would otherwise result in damage to biomolecules.<sup>1</sup> In the case of a lipid (LH), peroxidation of polyunsaturated acyl chain components<sup>2</sup> leads to products that are responsible for membrane damage in cells<sup>3</sup> and modified uptake in lipoproteins that results in atherosclerosis.<sup>4,5</sup> The chemical process of lipid peroxidation (Scheme 1) is a free radical chain reaction initiated by hydrogen atom abstraction from the allylic group of a polyunsaturated fatty acyl chain to produce a carbon-centred free radical (L) which reacts with molecular oxygen to form a propagating lipid peroxy free radical (LOO•).<sup>2</sup> Chain breaking antioxidants, of which the most important are the molecules comprising the vitamin E (tocopherol and tocotrienol) group, intercept the propagating lipid peroxy radical and inhibit the peroxidation process as indicated in Scheme 1.<sup>6,7</sup> The resulting tocopheroxyl radical is relatively stable and unreactive and so cannot propagate the chain reaction in the same way as LOO•.

Scheme 1 The free radical chain mechanism of lipid (LH) oxidation involving lipid (L•) and lipid hydroperoxides (LOO•) radicals as intermediates, and the role of tocopherols as chain-breaking antioxidants.



$\alpha$ -Tocopherol (R = -phytyl in Scheme 1) is the most active member of the vitamin E group and associates through the hydrophobic phytyl chain with membranes and lipoproteins wherein it exerts its antioxidant activity.<sup>8,9</sup> In order to facilitate investigation in aqueous solution Trolox C (R = -COOH), a water soluble  $\alpha$ -tocopherol analogue, has been widely studied. The absorption spectrum of the tocopheroxyl radical cation from Trolox C peaks 470nm, and shifts to 430 - 440 nm for the corresponding neutral radical.<sup>10,11 12</sup> The radical cation of the related cationic water soluble analogue MDL73404 (R =  $-(\text{CH}_2)_3\text{N}(\text{CH}_3)_3^+$ ) has a pK<sub>a</sub> of -1.4 as determined by transient absorption spectroscopy with laser flash photolysis.<sup>12</sup> Nanosecond flash photolysis of Trolox C in aqueous solution and of  $\alpha$ -tocopherol in SDS micelles shows formation of the neutral tocopheroxyl radical and the hydrated electron,<sup>13,15</sup> suggesting that the initial photoionization is rapidly followed by deprotonation, equation (1), on a sub-nanosecond timescale:



In acetonitrile the radical cation is more persistent and can readily be observed on a microsecond timescale.<sup>15</sup> In contrast, in methanol only the neutral radical is formed suggesting that in this less polar solvent only homolytic -OH bond breakage occurs. Therefore photoionization occurs as a result of high solvent polarity when the radical cation and electron are strongly solvated, and deprotonation is fast in the presence of a proton acceptor such as water. The contrast between photoionization in polar media and homolytic bond breaking in less polar solvents mirrors the possible mechanisms of concerted electron/proton transfer or hydrogen atom transfer in the antioxidant reaction of vitamin E. Photolysis therefore offers an opportunity

to study a half-reaction of the vitamin E reaction and in particular to measure the acidity and kinetics of proton loss from the tocopheroxyl radical cation.

Time-resolved Raman spectroscopy (TR<sup>3</sup>) of tocopherol photoionization has been performed in the nanosecond and picosecond time domains.<sup>12,14</sup> The advantage of TR<sup>3</sup> is that it provides a unique molecular specific fingerprint and by using a Raman excitation wavelength matching the electronic absorption of the molecule of interest, is able to provide a high contrast between solvent and solute species. This latter point has no equivalent in the complementary technique of infrared spectroscopy. Therefore TR<sup>3</sup> is well suited to the study of  $\alpha$ -tocopheroxyl cation and neutral radicals that are partially spectrally obscured in transient absorption spectra by the intense solvated electron absorption that is generated immediately following the photolyzing laser pulse. However, TR<sup>3</sup> studies are limited in time resolution to a few picoseconds because of the need to compromise between time resolution (duration of the probe laser pulse) and spectral resolution.<sup>16</sup> This limits temporal resolution to *ca.* 3 ps in order to maintain reasonable spectral resolution at *ca.* 15 cm<sup>-1</sup> and therefore picosecond TR<sup>3</sup> is unable to effectively resolve the initial stages of the photoionization and also potential reactions of excited states and radical species as they undergo proton loss due to a change in the pK<sub>a</sub> of the phenolic proton in going from the ground to excited and radical states. Furthermore the competing process of geminate recombination of the solvated electron and the ionized tocopheroxyl radical cation cannot be resolved. Femtosecond stimulated Raman spectroscopy (FSRS)<sup>17,18</sup> offers improved time resolution that is realized by the temporal nature of the overlap of two coherent optical fields from a picosecond Raman pump pulse,  $\omega_p$  and a femtosecond white-light continuum (the Raman probe pulse),  $\omega_s$ . A full review of FSRS has been given recently.<sup>19</sup> Briefly, when  $\omega_p$  and  $\omega_s$  are incident on the sample they drive a molecular vibration of frequency,  $\omega_v$ , equal to  $\omega_p - \omega_s$ . The

Stokes Raman transitions of the sample result in a net attenuation of the pump beam and net gain in the probe beam intensities. The evolution of the system can be described by coupled wave equations in which the pump and Stokes fields, also referred to as the gain side, are coupled parametrically by the polarization response of the sample. The gain of the Stokes field is determined by the third order Raman susceptibility,  $\chi^3_R$ , which is directly proportional to the spontaneous Raman cross section,  $dQ/d\Omega$ , and the derived polarizability tensor,  $d\alpha/dQ$ . The collected Raman spectrum extends across the bandwidth of the Raman probe beam and the temporal resolution in generating the eventually recorded vibrational coherence is determined by the cross correlation of the activating pump and Raman probe laser beams, here on the order of 200 fs. Finally for the reported time-resolved studies the FSRS Raman pump/probe beam pair is preceded by a photolytic UV pulse. For the water soluble  $\alpha$ -tocopherol analogue Trolox C (Scheme 1) we have chosen a resonant Raman pump pulse tuned within the absorption envelope of the Trolox radical cation and neutral radicals, at 430 and 470 nm respectively.

## **EXPERIMENTAL**

The experiments were performed using the 'ULTRA' laser system at the Science and Technology Facilities Council Rutherford Appleton Laboratory. The capabilities of the ULTRA instrument are described in detail elsewhere.<sup>20</sup> The instrument benefits from having synchronized picosecond and femtosecond laser sources avoiding the need to produce the picosecond pulse by bandwidth narrowing.<sup>21,22</sup> Briefly, a dual chirped-pulse amplified titanium:sapphire laser operating at 10 kHz repetition rate produced 40 fs and 2 ps duration pulsed outputs at a wavelength of 800 nm. The UV excitation pulse was produced by third harmonic generation of the 800 nm output of the amplifier with  $\sim$  50 fs duration at 266 nm, or at 290 nm with mixing

with a tunable OPA output. Samples were irradiated with a 1  $\mu\text{J}$ , 100  $\mu\text{m}$  diameter beam, polarized at the magic angle to and overlapped with the probe beams.

For TA and FSRS, a white-light continuum (WLC) in the UV to near IR was generated by focusing a portion of the 40 fs, 800 nm light into either a 2 mm thick sapphire or calcium fluoride plate. The continuum was split 50/50 for reference and probe with the probe beam passing through the sample, where it was focused to  $\sim 50 \mu\text{m}$ . For FSRS experiments, the Raman pump beam was generated through optical parametric amplifier mixing of the 800 nm, 2 ps duration output, which was spatially (100  $\mu\text{m}$  focused spot size) and temporally overlapped with the WLC at the sample. We have chosen a resonant Raman pump pulse tuned within the absorption envelope of the Trolox C radical cation and neutral radicals, at 430 and 470 nm respectively. Probe and reference spectra were recorded shot-to-shot on 512 element silicon array detectors.

For TRIR work the mid-IR probe pulse was generated using  $\sim 0.4 \text{ mJ}$  of the 800 nm femtosecond output to pump an optical parametric amplifier, followed by difference frequency mixing of the signal and idler components. The mid-IR probe output pulses had  $\sim 500 \text{ cm}^{-1}$  bandwidth and  $\sim 50 \text{ fs}$  pulse duration. The UV pulses were polarized at a magic angle to the IR probe laser polarization. Probe and reference spectra were recorded shot-to-shot on mercury cadmium telluride array detectors. The overall instrument response time was  $<200 \text{ fs}$ . The sample in solution was placed between two 25 mm diameter  $\text{CaF}_2$  plates in a Harrick cell. The cell was raster-scanned to limit irradiation of the sample by multiple pulses. The optical path of the sample between the two windows was controlled using a PTFE spacer 400  $\mu\text{m}$  for UV-Vis and FSRS and 200 to 300  $\mu\text{m}$  for TRIR. All solutions were flowed using a peristaltic pump.

Changes in probe spectra were monitored as a function of the time difference between the UV photolysis pulse and the probe pulse. Ground-state FTIR spectra were recorded using a Nicolet Avatar 360 spectrometer.

Trolox C,  $\alpha$ -tocopherol and methanol-d<sub>4</sub> were obtained from Aldrich. MDL73404 was a gift from Dr F. Bolkenius. Solutions of Trolox C and MDL73404 (from 1.5 to 7.5 mM) were prepared in H<sub>2</sub>O or D<sub>2</sub>O containing sodium phosphate buffer (50 mM, pH or pD = 7.1) or otherwise as indicated.

## RESULTS AND DISCUSSION

### Transient absorption (TA) spectra

Figure 1 shows the transient absorption spectra over a series of pump-probe delay times after photolysis of a solution of Trolox C (1.5 mM) in buffered D<sub>2</sub>O with a 290 nm pump pulse (200 fs resolution, 0.013 J cm<sup>-2</sup>). The spectra reveal a number of overlapping absorption bands of the various intermediates produced by photoexcitation of Trolox C. At the earliest time (1 ps) the spectrum contains absorption maxima at 560 nm and <380 nm. Absorbance at 600-680 nm increases at times up to 25 ps, and subsequently decays before finally reaching a constant value on the nanosecond timescale. The species responsible for the 560 and <380 nm transient absorptions is tentatively assigned to the excited singlet state (S<sub>1</sub>) that is the initial product of photoexcitation. From fluorescence quantum yield measurements, the lifetime of the excited state of Trolox C in water is estimated at ~ 15 ps (see Supplementary Information). The absorption spectrum in the long wavelength region (up to 680 nm) is attributed to the hydrated electron ( $\lambda_{\text{max}}$  706 nm in D<sub>2</sub>O)<sup>23</sup> and is similar to that observed by nanosecond flash photolysis of  $\alpha$ -tocopherol in micellar solutions.<sup>13,15</sup> As the hydrated electron absorption increases from 1 to 25

ps, there is evidence of a parallel growth in absorbance at 460-470 nm which corresponds to the absorption maximum of the tocopheroxyl radical cation, as observed for MDL74030 in acidic aqueous solution<sup>12</sup> and  $\alpha$ -tocopherol in MeCN and some other solvents.<sup>15,24</sup> The radical cation absorption subsequently decays at pump-probe delays longer than 25 ps and is replaced by a peak and shoulder at 400-440 nm characteristic of the Trolox C neutral radical.<sup>10,15</sup> This absorption then remains at a constant intensity on the nanosecond timescale. Whilst the characteristic signature of several different photolysis products may be identified from these spectra, their individual rates of formation and decay are difficult to evaluate due to the overlapping nature of their absorption spectra. A typical example of an absorbance transient at a single wavelength (in this case 470 nm) exhibits a prompt ( $< 1$  ps) formation of absorbance followed by a growth in absorbance with  $\tau = 15.6 \pm 2.7$  ps, followed by a decay with  $\tau = 60.8 \pm 12.3$  ps (Figure 1, inset). Similar time constants were obtained at wavelengths between 430 nm and 670 nm, although at 670 nm the initial prompt absorption attributed to  $S_1$  is absent. Equivalent time constants in  $H_2O$  are shown in Table 1.

**TABLE 1:** Summary of kinetics for transient formation and decays from transient absorption and FSRS measurements

<b>Transient Absorption Kinetics at 470 nm</b>			
Trolox C in $H_2O$			
Formation tau	5.3 ( $\pm$ 1.0) ps	$k_H/k_D$ (formation)	
Decay tau	30.8 ( $\pm$ 2.9) ps	2.9 ( $\pm$ 0.3)	
Trolox C in $D_2O$			
Formation tau	15.6 ( $\pm$ 2.7) ps	$k_H/k_D$ (decay)	
Decay tau	60.8 ( $\pm$ 12.3) ps	2.0 ( $\pm$ 0.2)	
<b>FSRS - Kinetics Raman Band</b>			
Trolox C in $H_2O$	1589 $cm^{-1}$	1485 $cm^{-1}$	
Formation tau	7.6 ( $\pm$ 2.3) ps	22.5 ( $\pm$ 2.21) ps	
Decay tau	42.7 ( $\pm$ 16.7) ps		
Trolox C in $D_2O$	1607 $cm^{-1}$	1494 $cm^{-1}$	1596 $cm^{-1}$
Formation tau	11.8 ( $\pm$ 6.1) ps	-	-
Decay tau	79.6 ( $\pm$ 30.0) ps	83.4 ( $\pm$ 21.5) ps	81.2 ( $\pm$ 19.7) ps

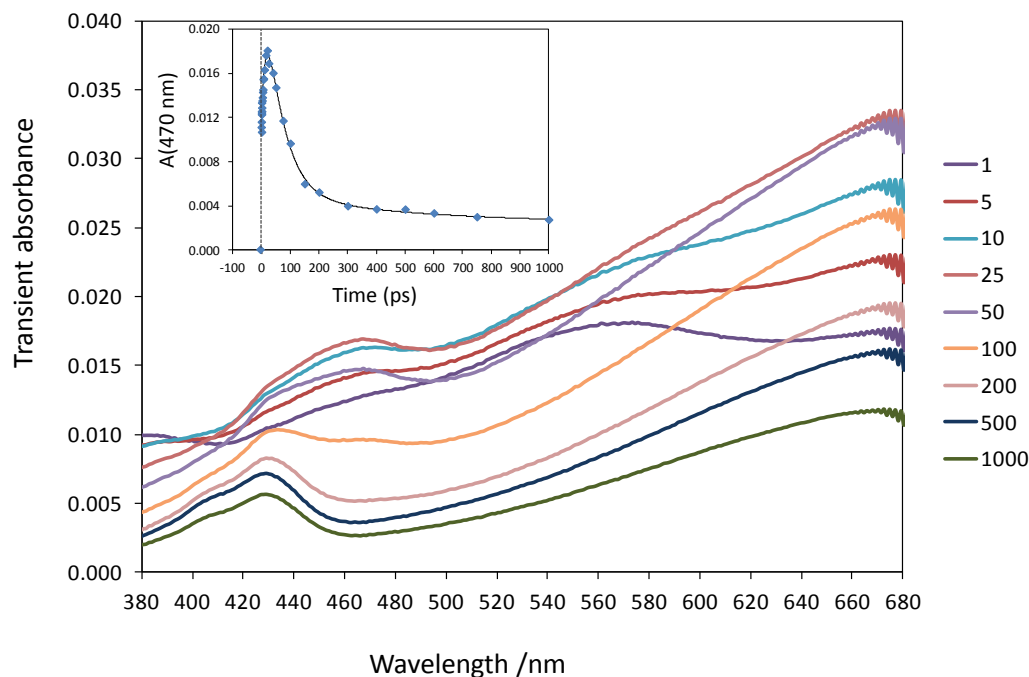
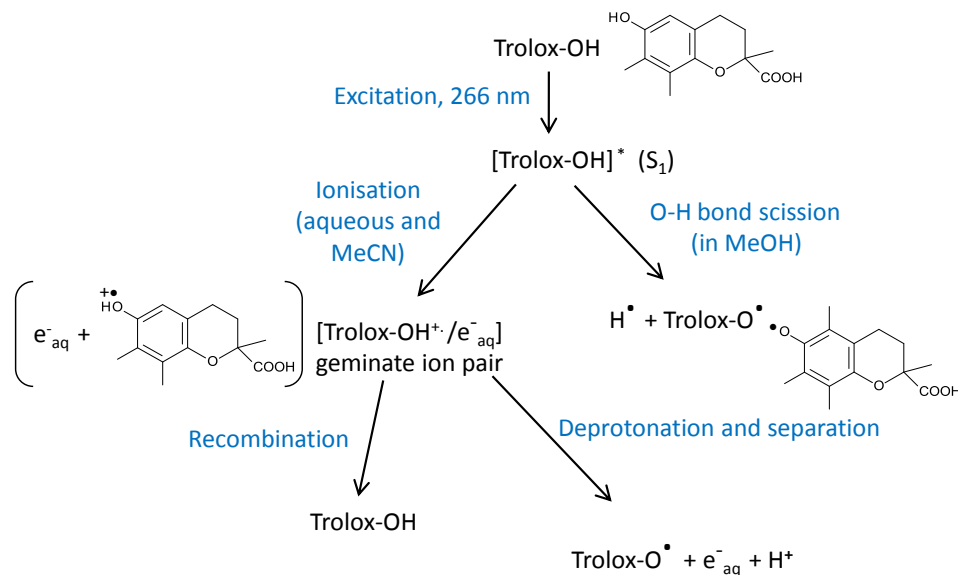


Figure 1 Transient absorption spectra from femtosecond photolysis at 290 nm ( $1 \mu\text{J}/\text{pulse}$ ) of Trolox C (1.5 mM) in  $\text{D}_2\text{O}$  containing phosphate buffer (50 mM) at pD 7.1 with a probe pathlength of 1.5 mm and pump-probe delays between 1 ps and 1,000 ps. **Inset:** Picosecond kinetics of absorption formation and decay at 470 nm.



Scheme 2 Proposed mechanisms of photoexcitation and photoionization of Trolox C, showing solvent dependence of geminate ion pair formation and homolytic -O-H bond dissociation.

The photolysis of the phenolate ion has recently been studied on an ultrafast timescale by transient absorption spectroscopy.<sup>25</sup> Similar electron ejection was observed and transient assigned to the phenolate excited state at 515 nm was reported.

Figure 2 shows the effect of increasing HCl concentration on the transient absorption at 680 nm. The residual absorption at times >200 ps is scavenged by HCl with a second order rate constant of *ca.*  $10^{10} \text{ dm}^3 \text{ mol}^{-1} \text{ s}^{-1}$  consistent with literature values for reaction of  $e^-_{\text{aq}}$  with  $\text{H}^+$ <sup>26</sup>, and confirms the identity of this residual absorption as that of the hydrated electron as previously observed in nanosecond experiments where a one-photon dependence has been established.<sup>13,15</sup>

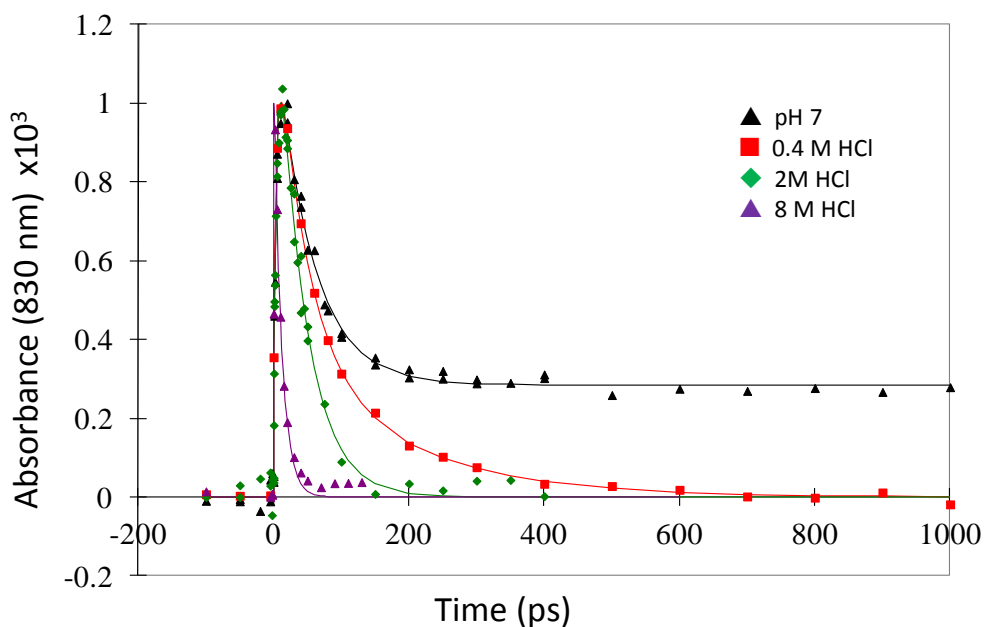


Figure 2 Absorption transients at 680 nm after femtosecond excitation at 266 nm of MDL73404 (4 mM) in phosphate buffered (20 mM) H<sub>2</sub>O and in H<sub>2</sub>O solutions containing increasing concentrations of HCl as indicated.

As shown in Scheme 2, the transient absorption results suggest that both the radical cation and hydrated electron evolve through autoionization of a precursor state such as S<sub>1</sub> in a process that

is accompanied by solvation of both products, as similarly proposed for phenolate by Chen et al.<sup>25</sup> The rate of formation of the radical cation is comparable with that of vibrational relaxation of a typical excited state. The kinetic isotope ratio ( $k_H/k_D$ ) for the formation of the radical cation and hydrated electron is  $2.9 \pm 0.3$  and is consistent with the role of water in the solvation process. The initial formation of the radical cation and hydrated electron, is followed by a second phase in which only a fraction (estimated at *ca.* 80% in D<sub>2</sub>O) of the hydrated electron and radical cation signals decay with a time constant of *ca.* 60 ps in D<sub>2</sub>O as described above. This partial decay appears to relate to the recombination of a geminate radical-ion pair. The limited recombination may be due to either a) separation of the ion pair so that normal diffusion kinetics take over after the first 500 ps in D<sub>2</sub>O, or b) deprotonation of the radical cation resulting in a lowering of reactivity of the ion pair. Although the radical cation has a substantially higher reduction potential than that of the neutral radical (480 mV)<sup>27</sup> by about 400 mV<sup>28,29</sup>, reaction of the hydrated electron with the latter will remain very strongly exergonic and so the first explanation is preferred. Also favoring a) is that deprotonation will reduce the attractive interaction of the geminate ion pair and facilitate separation. This conclusion is supported by the observation of geminate ion pair between the hydrated electron and neutral phenoxyl radical by Chen et al.<sup>25</sup> The recombination phase of the reactions observed in Figures 1 and 2 has a  $k_H/k_D$  ratio of  $2.0 \pm 0.2$ , again suggesting the involvement of a proton transfer or solvation, in this instance consistent with proton transfer to solvent as would occur in the deprotonation reaction (Scheme 2). Further investigation requires a technique that will independently allow the formation and decay of the cation and neutral radicals to be resolved spectrally and temporally.

### Femtosecond Stimulated Raman Spectroscopy (FSRS)

FSRS was used to investigate the reactions described above using actinic pulses at 266 or 290 nm and a Raman pump at 435-450 nm to be on resonance with the absorption spectra of the neutral and cation radicals of Trolox C. Figure 3 shows the results from Trolox C (7.5 mM) in D<sub>2</sub>O with the Raman pump at 435 nm. The time-resolved spectra in Figure 3A show the initial formation of a Raman gain band at times up to 50 ps, with a peak at 1607 cm<sup>-1</sup>. This compares with a Raman shift of 1620 cm<sup>-1</sup> previously reported for the tocopheroxyl radical cation of MDL74303 in 10 M HCl and assigned to the  $\nu_{8a}$  C=C ring stretching mode.<sup>12</sup> At pump-probe delays longer than 10 ps, the spectra show the emergence of a second band at 1494 cm<sup>-1</sup>.

Simultaneously the original band shifts to slightly lower frequency at 1596 cm<sup>-1</sup>. The bands observed at the longer time delays are similar to those of the neutral tocopheroxyl radical previously reported and correspond to the C-O  $\nu_{7a}$  (1492 cm<sup>-1</sup>) and  $\nu_{8a}$  ring C=C (1600 cm<sup>-1</sup>) modes of the Trolox C neutral radical. Compared with the previous picosecond TR<sup>3</sup> spectra obtained for photolysis of Trolox C<sup>14</sup>, these spectra exhibit improved spectral resolution with clear separation of the  $\nu_{7a}$  and  $\nu_{8a}$  bands of the neutral radical species.

Figure 3B shows the kinetics obtained by fitting the spectra to three Gaussian bands and plotting the integrated intensity of each band *versus* time. The 1607 cm<sup>-1</sup> band of the radical cation grows in with a time constant of  $11.8 \pm 6.1$  ps and then decays with a lifetime of  $79.6 \pm 30.0$  ps (see Table 1). These are in good agreement with lifetimes determined from transient absorption experiments. The data also allows time constants of  $83.4 \pm 21.5$  and  $81.2 \pm 19.7$  ps to be obtained for the formation of the neutral radical bands at 1494 and 1596 cm<sup>-1</sup> respectively, again agreeing well with the transient absorption data. Similar data for the reactions in H<sub>2</sub>O are

shown in Figure 4 and the kinetics in Table 1, although in this case the two bands in the region of  $1600\text{ cm}^{-1}$  could not be satisfactorily resolved, and the results were obtained at each frequency. As in the transient absorption results, the rates obtained by FSRS in  $\text{H}_2\text{O}$  are faster by about a factor of two compared with those in  $\text{D}_2\text{O}$ .

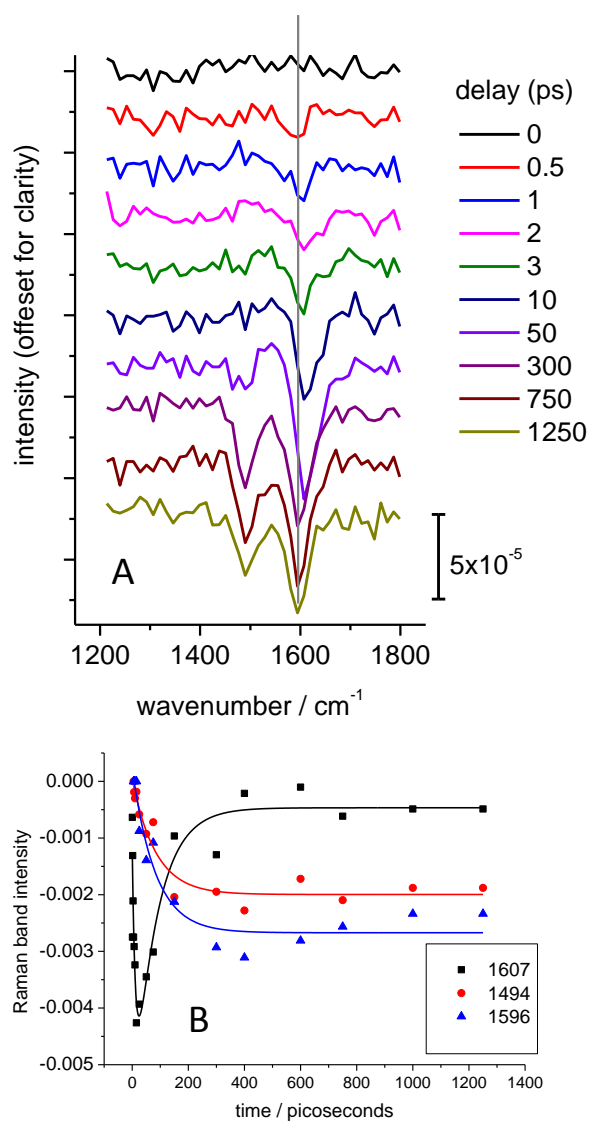


Figure 3 A: Femtosecond stimulated Raman spectra from solutions of Trolox C (7.5 mM) in phosphate buffered (50 mM)  $\text{D}_2\text{O}$  solution at pD 7.1 measured using a photolysis pulse wavelength of 266 nm and a 435 nm Raman pump at the indicated pump-probe delays (ps). The plots show FSRS intensity gain in the downwards direction. Panel B shows the derived kinetic traces at 1494 (●), 1596 (▲) and 1607 (■)  $\text{cm}^{-1}$  using the full data set.

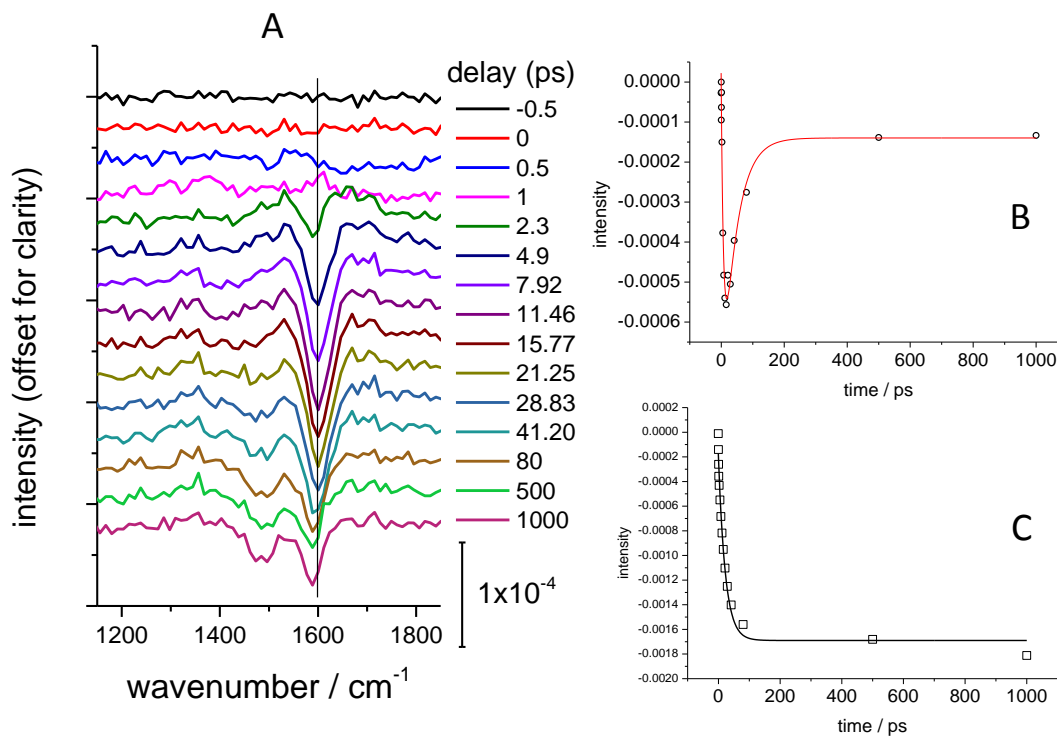


Figure 4 A: Femtosecond stimulated Raman spectra from solutions of Trolox C (7.5 mM) in phosphate buffered (50 mM) H<sub>2</sub>O solution at pH 7.1 measured using a photolysis pulse wavelength of 266 nm and 450 nm Raman probe and the indicated delays (ps). The plots show FSRS intensity gain in the downwards direction. Panels B and C show the derived kinetic traces at 1589 and 1485 cm<sup>-1</sup> respectively using the full data set.

The FSRS data now clearly show that it is the deprotonation of the radical cation that is controlling the decay of the hydrated electron. After the deprotonation reaction is complete, the hydrated electron no longer decays on the timescale of Figure 1 (i.e. up to 1 ns). Since on energetic grounds the neutral radical would be expected to react rapidly with the hydrated electron within a radical pair, it is therefore concluded that separation of the geminate ion pair is also determined by this deprotonation rate with the electron becoming free as the proton is transferred from the radical cation to solvent, as summarized in Scheme 2. The rate of proton loss from the Trolox radical cation is consistent with the measured rates of proton loss in the

region of  $2 \times 10^{10} \text{ s}^{-1}$  ( $\tau$  50 ps) from excited photoacids with  $\text{pK}_a$  values in the region of -1,<sup>30,31</sup> similar to that for the tocopheroxyl radical cation.<sup>12</sup> By analogy, Trolox may be described as a “radical-acid”. The relative stability of the tocopheroxyl radical in non-aqueous media such as hexane<sup>28</sup> and acetonitrile<sup>24</sup> is therefore a result of the inability of these solvents to accept a proton.

### **Time-resolved infrared (TRIR) studies.**

The picosecond TA and FSRS studies described above clearly show the evolution of radical states of Trolox C. In addition the TA spectra from photoexcitation of Trolox C in aqueous solution contain a short-lived broad transient absorption at 560 nm that is tentatively assigned to the initially excited electronic state. In order to complement these studies the TRIR spectra of  $\alpha$ -tocopherol and Trolox C have been investigated. In contrast to the photoionization of Trolox C in aqueous media described above, Zhang *et al.* have reported that in methanol solutions photolysis of  $\alpha$ -tocopherol proceeds through direct dissociation of the –O-H bond to produce  $\alpha\text{-Toc-O}^\cdot$ .<sup>15</sup> TRIR spectra of  $\alpha$ -tocopherol in methanol-d<sub>4</sub> (Figure 5) show that immediately following excitation ( $\leq 1$  ps) bleaching is observed of the ground state absorptions at 1460 and 1420  $\text{cm}^{-1}$  previously attributed to phenyl skeletal modes and at 1264  $\text{cm}^{-1}$  resulting from methyl symmetric bending.<sup>32</sup> Simultaneously an intense band at 1349  $\text{cm}^{-1}$  is formed. On the basis of the lifetime of this species (*vide infra*) this is assigned to the excited singlet state and most likely corresponds to a ring mode of the chroman system. This band rapidly shifts to 1354  $\text{cm}^{-1}$  with a time constant of  $10 \pm 2$  ps (Figure 5C), following which it decays with a lifetime of  $1.2 \pm 0.2$  ns (Figure 5B). The fast shift is ascribed to relaxation of the initial vibrationally excited  $S_1$  state and the slower nanosecond decay corresponds to the fluorescence lifetime of  $\alpha$ -tocopherol in MeOH reported as 1.21 ns.<sup>33</sup> A second band at 1520  $\text{cm}^{-1}$  shows a decay with a similar nanosecond time constant

and is proposed to be associated with the phenolic C-O stretch of the excited state. Close inspection of this feature after a pump-probe delay of 3 ns reveals a residual absorption at 1502  $\text{cm}^{-1}$  that corresponds to the C-O  $\nu_{7a}$  mode of the  $\alpha$ -tocopherol  $\alpha$ -Toc-O $\cdot$  radical in methanol.<sup>12</sup>

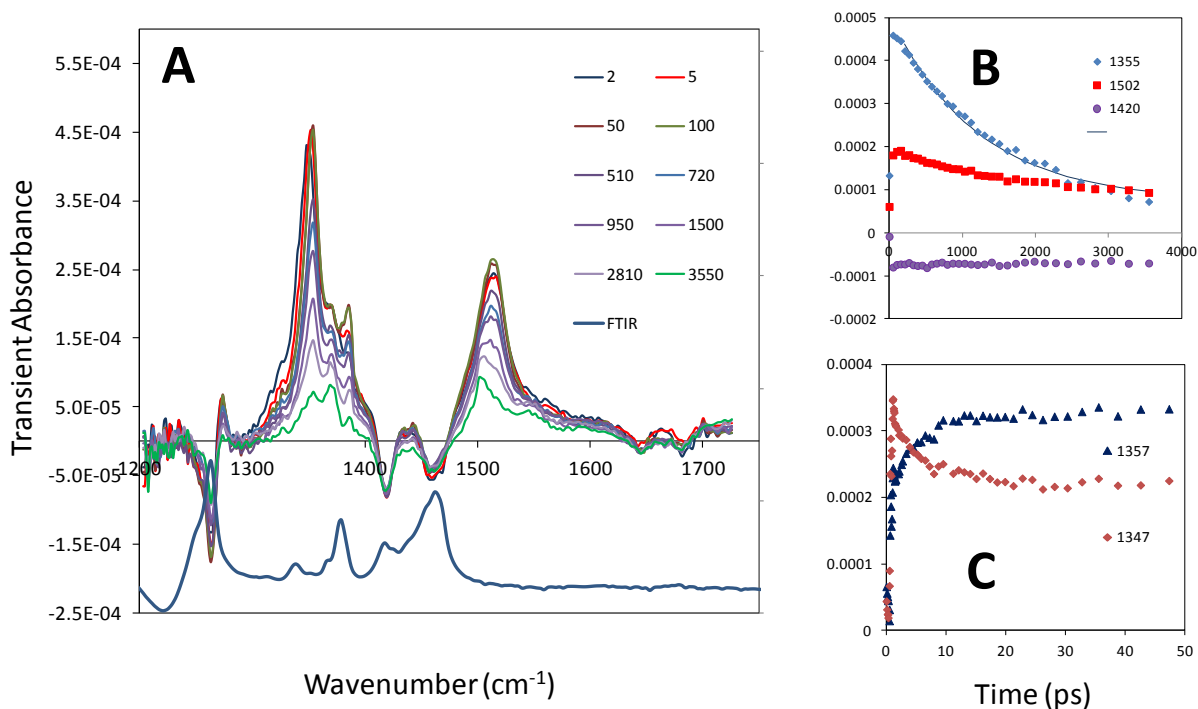


Figure 5 Picosecond time-resolved infrared (TRIR) spectra (A) from photolysis at 266 nm of  $\alpha$ -tocopherol (60 mM) in methanol-d<sub>4</sub>. The FTIR spectrum of  $\alpha$ -tocopherol is shown for comparison. Panels B and C shows kinetic data at nanosecond and picosecond timescales respectively from the complete data set at selected wavenumbers as indicated.

No band corresponding to the C=C  $\nu_{8a}$  mode at 1595  $\text{cm}^{-1}$  of the neutral radical is observed and it is concluded that for the neutral radical this mode is infrared inactive. However the absence of the radical cation C=C  $\nu_{8a}$  band at around 1620  $\text{cm}^{-1}$ , which is observed for Trolox in D<sub>2</sub>O (*vide infra*), supports the proposed direct homolysis of the -O-H bond of  $\alpha$ -tocopherol in methanol as previously inferred by Zhang *et al.* from nanosecond photolysis studies.<sup>15</sup> Figure 5 also shows that whilst the excited state transients at 1354 and 1520  $\text{cm}^{-1}$  have decayed to ~15%

of their original intensities at 3 ns delay, the bleach of the ground state band at  $1420\text{ cm}^{-1}$  remains at  $\sim 85\%$  of its original value. Similarly the transient absorption of the tocopheroxyl neutral radical at  $1506\text{ cm}^{-1}$  reaches a relatively constant value at 3 ns delay (Figure 3B). The lack of recovery in the ground state bleach over the timescale of the electronic excited state decay indicates that formation of the tocopheroxyl radical is relatively efficient in methanol. For vitamin E in methanol the reported quantum yield of fluorescence is  $0.09$ <sup>33</sup>, whilst the singlet oxygen yield (originating from the triplet state) is  $0.17$ .<sup>34</sup> Together, fluorescence, triplet state and radical formation appear to be the only major processes resulting from the initial excited singlet state.

TRIR spectra from photolysis of Trolox C in methanol-d<sub>4</sub> are shown in Figure 6. Bands identified above as originating from the excited state are observed at  $1350\text{ cm}^{-1}$  and  $1517\text{ cm}^{-1}$  and in which the initial vibrational cooling during the first 10 ps in the  $1340\text{-}1350\text{ cm}^{-1}$  region is seen. The transient absorption at  $1351\text{ cm}^{-1}$  decays as a biexponential with lifetimes of  $7.0 \pm 0.6$  ps and  $73 \pm 11$  ps. The faster component is consistent with vibrational cooling, whereas the slower decay is taken as the excited state lifetime. The second excited state band at  $1520\text{ cm}^{-1}$  again decays to reveal a long-lived transient absorption at  $1508\text{ cm}^{-1}$  belonging to the neutral radical. Compared with the TRIR spectrum from vitamin E discussed above, the Trolox C TRIR spectrum in methanol-d<sub>4</sub> contains an additional bleach in absorbance at  $1725\text{ cm}^{-1}$  which is the expected frequency for the carbonyl stretch of the undissociated carboxylic acid group<sup>35</sup> in the ground state. The  $1725\text{ cm}^{-1}$  bleach initially recovers with a lifetime of  $6.3 \pm 0.3$  ps, leaving a static bleach on the timescale observed. Another additional band in the TRIR spectrum of Trolox C in methanol-d<sub>4</sub> is a weak transient at *ca.*  $1630\text{ cm}^{-1}$ . This is at slightly too high wavenumber

for the radical cation C=C  $\nu_{8a}$  band vibration and may instead be the transient due to the carboxylic acid group in the excited state with lower bond order and extinction coefficient.

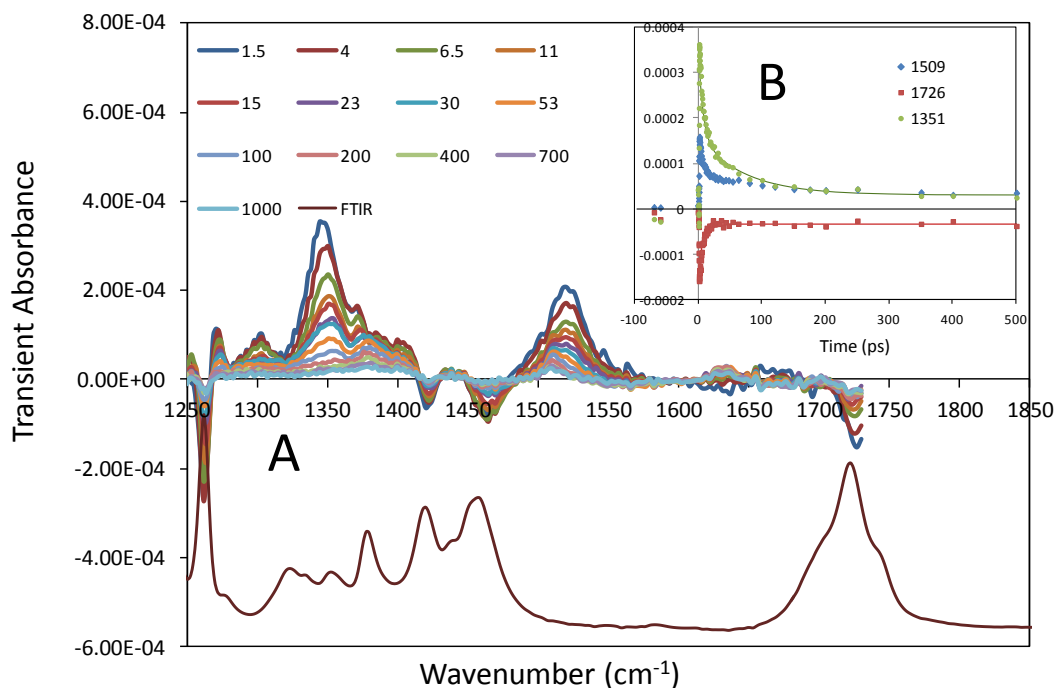
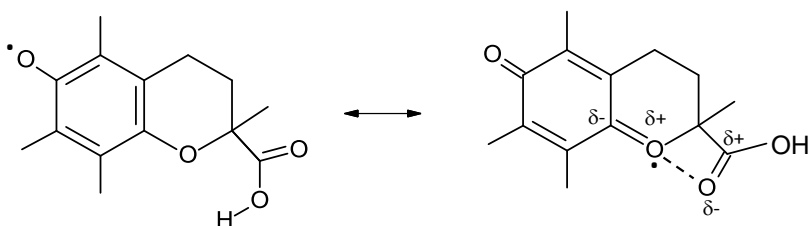


Figure 6 Picosecond time-resolved infrared (TRIR) spectra (A) from photolysis at 266 nm of Trolox C (30 mM) in methanol-d<sub>4</sub>. Panel B shows kinetic data from the complete data set at selected wavenumbers as indicated.

A major difference between the TRIR spectra of  $\alpha$ -tocopherol and Trolox in methanol-d<sub>4</sub> is the large difference in the recovery of the bleached ground state bands. In  $\alpha$ -tocopherol it was noted that there was less than 15% recovery whilst in Trolox C recovery occurs on an approximately 7 ps timescale and amounts to about 80%. Since dissociation occurs from the S<sub>1</sub> excited state, the longer lifetime of  $\alpha$ -tocopherol leads to a much larger yield of the neutral radical as compared with Trolox C in methanol-d<sub>4</sub>. It is interesting that the carboxylic acid group is seen to report the conversion of Trolox C to the excited state and neutral radical species. It is well known that

the unpaired electron in the neutral radical species is delocalised to the chroman oxygen atom and that this serves to stabilise the radical in order to reduce its reactivity and increase the chain-breaking activity of vitamin E.<sup>36</sup> Scheme 3 suggests how the  $\delta^+$  charge of the chroman oxygen atom in the resonance hybrid might interact with the carboxylic group so that the latter responds to radical formation (*vide infra*).



Scheme 3 The proposed interaction of the carboxylic acid group with the chroman oxygen in the quinoidal canonical structure of the neutral Trolox C radical resulting from the electron delocalization proposed by Burton and Ingold<sup>36</sup>.

The TRIR spectra of Trolox C in D<sub>2</sub>O (Figure 7) show similar evidence of the excited state from transient absorptions at *ca.* 1360 and 1510 cm<sup>-1</sup> that decay with a lifetime of between 30 and 40 ps (Table 2). This short lifetime of the excited state of Trolox C in D<sub>2</sub>O is consistent with the much lower fluorescence quantum yield compared with that of  $\alpha$ -tocopherol in MeOH. Since the carboxylic acid group (pK = 3.89)<sup>37</sup> is deprotonated to the carboxylate at pD 7 the ground state carbonyl IR absorption shifts to 1580 cm<sup>-1</sup> together with the corresponding bleach in the TRIR spectrum. The inset kinetic traces to Figure 7 show that whilst the transient singlet state bands at 1366 and 1391 cm<sup>-1</sup> essentially decay to zero after 300 ps, there remains transient absorption at 1505 cm<sup>-1</sup> at 1 ns resulting from the neutral radical, together with incomplete recovery of the bleach at 1575 cm<sup>-1</sup>. In addition a major new feature of the TRIR spectrum of Trolox C in D<sub>2</sub>O is the appearance of a strong band at 1605 cm<sup>-1</sup> not observed in the TRIR

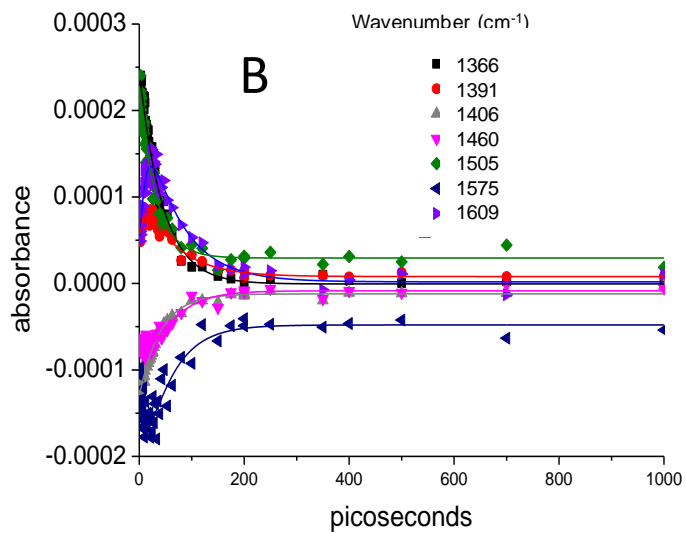
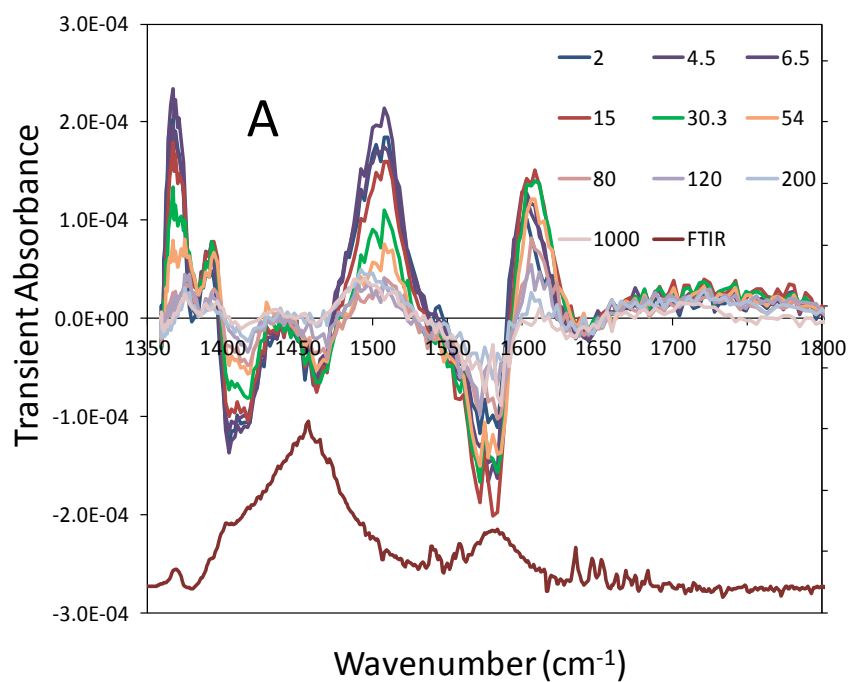


Figure 7 A:- Picosecond time-resolved infrared (TRIR) spectra from photolysis at 266 nm of Trolox C (7.5 mM) in D<sub>2</sub>O solution containing phosphate buffer (50 mM, pD 7.1). Panel B shows kinetic data from the complete data set at selected wavenumbers as indicated.

Wavenumber (cm <sup>-1</sup> )		Tau (ps)
1366	$\tau 2$ (decay)	44.7 ± 2.2
1391	$\tau 1$ (rise)	7.6 ± 2.0
	$\tau 2$ (decay)	64.5 ± 10.2
1406	$\tau 2$ (decay)	40.4 ± 2.3
1460	$\tau 1$ (rise)	21.9 ± 21.3
	$\tau 2$ (decay)	46.0 ± 27.7
1505	$\tau 2$ (decay)	32.1 ± 2.2
1575	$\tau 1$ (rise)	12.6 ± 7.0
	$\tau 2$ (decay)	50.3 ± 18.9
1609	$\tau 1$ (rise)	11.5 ± 2.2
	$\tau 2$ (decay)	67.2 ± 11.5

Table 2 – Kinetics of transient formation and decay in the TRIR spectra of Trolox C in D<sub>2</sub>O solution from the data in Figure 7

spectra of either  $\alpha$ -tocopherol or Trolox C in methanol-d<sub>4</sub>. This TRIR band is at the same TR<sup>3</sup> frequency as the C=C  $\nu_{8a}$  band of the radical cation in the vitamin E analogue MDL7304<sup>12</sup>, and observation of this species in the TRIR spectra is consistent with evidence from the TA and FSRS spectra in aqueous solution. Moreover this band displays an initial increase in intensity with a time constant of 11.5 ± 2.2 ps that is similar to that for the formation of the radical cation observed in both the TA and FSRS experiments in D<sub>2</sub>O (Table 1). The decay of the radical cation band at 1609 cm<sup>-1</sup> in the TRIR spectrum (67 ± 11 ps) is similar to that in the FSRS spectrum in D<sub>2</sub>O (79.6 ± 12 ps). The bleach of the ground state of Trolox C in D<sub>2</sub>O at 1575 cm<sup>-1</sup> shows recovery with a similar time constant. However this recovery extends to only about 80% of the initial bleach and shows that eventual formation of the neutral tocopheroxyl radical (also observed here at later times within the envelope of the 1600-1620 cm<sup>-1</sup> band) is relatively inefficient. This is because of the ultrafast geminate radical cation and hydrated electron

recombination observed by all three spectroscopic techniques, compared with the direct formation of the neutral radical from  $\alpha$ -tocopherol in methanol.

### Quantum mechanical calculations

In order to describe possible interactions suggested by the TRIR spectra between the carboxylic acid group of Trolox C and the chroman oxygen atom (O(18)) as proposed in Scheme 3 (see Figure 8D for atom numbering used), quantum mechanical calculations of the energy of the neutral Trolox C radical, as in methanol solution, *versus* the O(18)-C(12)-C(14)-O(16) dihedral angle were undertaken. The calculations used DFT(BPW91) with 6-311G+(2d,p) basis in the Gaussian 09 package.<sup>38-40</sup> Solvent effects were considered using a polarizable continuum model (PCM) within the integral equation formalism (IEF-PCM). All calculations and optimizations were conducted on structures where labile protons had been replaced with deuterium atoms. The dihedral angle formed by O(18)-C(12)-C(14)-O(16) was altered from 0 to 360° in 30° increments and at each step the structure optimised in an IEFPCM methanol solvent field. The relative energies are shown in Figure 8 together with some key bond lengths. Two minima of similar energy occur corresponding to close approach of either of the carboxylic acid oxygen atoms to chroman O(18). In the first instance, at a dihedral angle of 0° the hydrogen atom H(35) of the carboxylic acid group attached to O(16) is oriented towards the chroman oxygen O(18) and close enough (2.0 Å) to form a hydrogen bond. For the second minimum at a dihedral angle of 180° the carbonyl oxygen of the carboxylic acid group, O(17), comes into proximity with the chroman O(18) atom. This corresponds to the situation depicted in Scheme 3 and arises through interaction of the  $\delta^-$  charge of O(17) with the  $\delta^+$  charge that develops on O(18) through electron delocalisation from the 2p<sub>z</sub> orbital of O(18) to the phenolic oxygen O(15) to form a quinoidal structure as proposed by Ingold *et al.* for vitamin E.<sup>36</sup> Both interactions are

calculated to have significant stabilisation to the extent of *ca.* 12 kcal mol<sup>-1</sup>. Corresponding changes in the phenolic C(6)-O(15) and carboxylic acid carbonyl C(14)-O(17) bond lengths are also shown in Figure 8. The phenolic C(6)-O(15) bond length shows a somewhat complex dependence on the O(18)-C(12)-C(14)-O(16) dihedral angle, with the shortest bond length corresponding to the least quinoidal-type structure at 0°. However a shallow minimum is also calculated in the region of 180° corresponding to the energy minimum described above. Significantly in relation to the TRIR results shown previously, the carbonyl C(14)-O(17) bond length changes from a minimum of 1.196 Å at an angle of 90° to a maximum of 1.205 Å at 180°. The increase in bond length is consistent with an increase in bond order and a reduction in the infrared frequency of the C(14)-O(17) bond, allowing a bleaching in the TRIR spectra as observed in Figure 6.

#### **Relevance to biochemical action of vitamin E as an antioxidant**

Combination of the TA and FSRS data shows that in both H<sub>2</sub>O and D<sub>2</sub>O the solvated electron absorption at > 600 nm decays at a similar rate to the decay of the radical cation and is matched to the formation of the neutral radical. Our results indicate that the recombination between the electron and the radical cation occurs at the same rate as deprotonation and separation of the geminate ion pair. The formation of the fully solvated neutral radical therefore depends on both the deprotonation of the radical cation and complete loss of the electron from within the columbic field, and the yield of solvated radical is 0.5 of the geminate -ion pair. Once in the bulk solution recombination reaction between the hydrated electron and neutral radical is unable to occur on the sub-microsecond timescale.

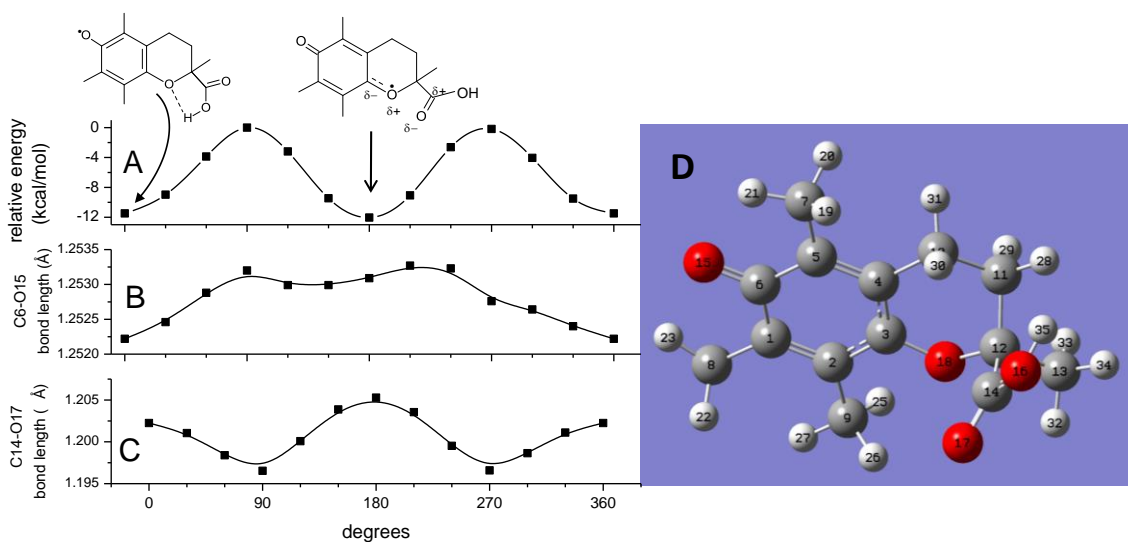
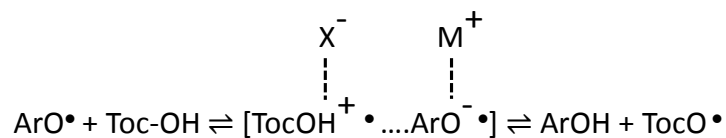


Figure 8 Various structural parameters for neutral Trolox C radical in methanol solution obtained from calculations varying the dihedral angle formed by O(18)-C(12)-C(14)-O(16). A) Relative energy differences from the maximum energy obtained for the 90° configuration (-529957.2 kcal/mol); B) Phenoxyl C(6)-O(15) bond length; C) Carboxylic acid carbonyl C(14)-O(17) bond length; D) Atom numbering. Also shown are the structures indicating configuration of the carboxylic acid group at dihedral angles of 0° and 180° as discussed in the text.

Our studies using FSRS and TRIR in the picosecond regime together with those of Razi Naqvi and co-workers<sup>15,24</sup> on the nanosecond and microsecond timescales complement the recent theoretical work of Alberto *et al.*<sup>41</sup> Using reaction energies calculated with quantum mechanical methods, they have considered two mechanisms of radical reactions with Trolox that are relevant to the current investigations, namely i) H-atom transfer (HT), and ii) single electron transfer (SET). [The radical addition reaction also considered by Alberto *et al.* is outside the scope of the present results whilst the “single proton loss electron transfer” (SPLET) reaction amounts only to reaction of that fraction of Trolox C in which the phenolic group is deprotonated under the particular solution conditions (less than  $10^{-4}$  at pH 7)]. In non-aqueous solvents such as a lipid environment, the calculations of Alberto *et al.* suggest that HT involving the phenolic group is the dominant mechanism for a range of free radicals including the highly reactive hydroxyl

radical, leading directly to tocopheroxyl neutral radical formation. Homolysis of the phenolic – OH bond is also the outcome of both the present picosecond TRIR experiments with Trolox in methanol and the microsecond photolysis experiments with vitamin E in methanol.<sup>15</sup> In contrast for Trolox C in neutral aqueous solution, SET is shown to be favorable for reaction of the hydroxyl radical but not for less reactive peroxy and alkoxy radicals, for which HT is calculated to remain the dominant mechanism. However the definition of the SET reaction for peroxy and alkoxy radicals by Alberto *et al.* leaves both products in non-equilibrium protonation states, and further coupling of deprotonation/protonation reactions may affect the overall energetics. In particular, the electron transfer process considered by Alberto *et al.* leaves the vitamin E radical in the protonated state, which the present results show will lose a proton on an ultrafast timescale at pH 7.

Within the context of  $\alpha$ -tocopherol as an antioxidant in biochemical systems, the postulated involvement of the radical cation in the transition state has been supported by experiments showing that the rate of reduction of aroxyl radicals by  $\alpha$ -tocopherol is increased by the presence of metal salts.<sup>42,43</sup> This effect was suggested to occur through stabilization of the transition state in which electron transfer creates the tocopherol radical cation – aroxyl anion transition state complex as shown in Scheme 4. Photoionization of tocopherols as shown here may be regarded as a half-reaction of the biochemical process. Our results show that due to the very high acidity of the tocopheroxyl radical cation, in the transition state (shown in Scheme 4) proton transfer would proceed extremely rapidly and the reaction may be conveniently be viewed as a concerted electron-proton transfer.<sup>42,43</sup>



Scheme 4 Transition state stabilization by metal salts in the reduction of aroxyl radicals (ArO·) by tocopherol as proposed by Kohno *et al.*<sup>43</sup>

## ACKNOWLEDGEMENTS

The authors acknowledge the Central Laser Facility, Science and Technology Facilities Council (STFC) for providing access to the experimental facilities. The work was jointly funded by STFC and the University of Salford.

Supporting Information Available: Calculated TRIR spectra and fluorescence quantum yields of Trolox C and vitamin E are reported. This material is available free of charge via the Internet at <http://pubs.acs.org>.

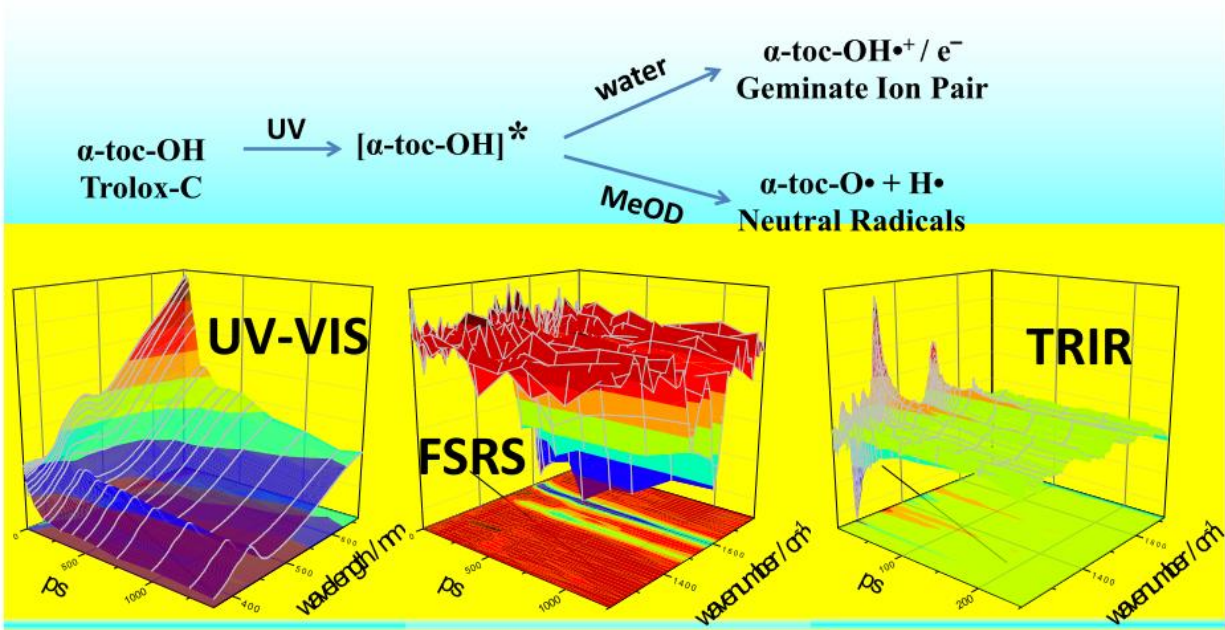
## REFERENCES

1. Halliwell, B.; Gutteridge, J.M.C. *Free Radicals in Biology and Medicine (4<sup>th</sup> Edition)*, OUP: Oxford, **2007**.
2. Choe, E.; Min, D.B. Chemistry and Reactions of Reactive Oxygen Species in Foods. *Crit. Rev. Food Sci.* **2006**, 46, 1-22.
3. Miki, M.; Tamai, H.; Mino, M.; Yamamoto, Y.; Niki, E. Free-radical Chain Oxidation of Rat Red Blood Cells by Molecular Oxygen and its Inhibition by alpha-Tocopherol. *Arch. Biochem. Biophys.* **1987**, 258, 373-380.
4. Esterbauer, H.; Gebicki, J.; Puhl, H.; Jurgens, G. The Role of Lipid Peroxidation and Antioxidants in Oxidative Modification of LDL. *Free Radic. Bio. Med.* **1992**, 13, 341-390.
5. Parthasarathy, S.; Steinberg, D.; Witztum, J.L. The Role of Oxidized Low-Density Lipoproteins in the Pathogenesis of Atherosclerosis. *Annu. Rev. Med.* **1992**, 43, 219-225.
6. Burton, G.W.; Ingold, K.U. Autoxidation of Biological Molecules. 1. The Antioxidant Activity of Vitamin E and Related Chain-breaking Phenolic Antioxidants in vitro. *J. Am. Chem. Soc.* **1981**, 103, 6472-6477.
7. Traber, M.G.; Atkinson, J. Vitamin E, Antioxidant and Nothing More. *Free Radic. Biol. Med.* **2007**, 43, 4-15.
8. Bisby, R.H. Interactions of Vitamin E with Free Radicals and Membranes. *Free Radical Res.* **1990**, 8, 299-306.
9. Marquardt, D.; Williams, J.A.; Kučerka, N.; Atkinson, J.; Wassall, S.R.; Katsaras, J.; Harroun, T.A. Tocopherol Activity Correlates with Its Location in a Membrane: A New Perspective on the Antioxidant Vitamin E. *J. Am. Chem. Soc.* **2013**, 135, 7523-7533.
10. Bisby, R.H.; Ahmed, S.; Cundall, R.B. Repair of Amino Acid Radicals by a Vitamin E Analogue. *Biochem. Biophys. Res. Co.* **1984**, 119, 245-251.
11. Davies, M.J.; Forni, L.G.; Willson, R.L. Vitamin E Analogue Trolox C - Electron Spin Resonance and Pulse Radiolysis Studies of Free Radical Reactions. *Biochem. J.* **1988**, 255, 513-522.
12. Parker, A.W.; Bisby, R.H. Time-resolved Resonance Raman Spectroscopy of  $\alpha$ -Tocopheroxyl and Related Radicals in Solvent, Micellar and Membrane Systems *J. Chem. Soc. Faraday T.* **1993**, 89, 2873-2878.
13. Bisby, R.H.; Parker, A.W. Reactions of the  $\alpha$ -Tocopheroxyl Radical in Micellar Solutions Studied by Nanosecond Laser Flash Photolysis. *FEBS Lett.* **1991**, 290, 205-208.

14. Towrie, M.; Gaborel, G.; Matousek, P.; Parker, A.W.; Shaikh W.; Bisby, R.H. Tuneable Picosecond Optical Parametric Amplifiers for Time-Resolved Resonance Raman Spectroscopy. *Laser Chem.* **1999**, 19, 153-159.
15. Zhang, Y.; Yousef, Y.A.; Li, H.; Melø, T.B.; Razi Naqvi, K. Comparison of the Photochemical Behaviours of alpha-Tocopherol and its Acetate in Organic and Aqueous Micellar Solutions. *J. Phys. Chem. A* **2011**, 115, 8242-8247.
16. Sahoo, S.K.; Umamathy, S.; Parker, A.W. Time-Resolved Resonance Raman Spectroscopy: Exploring Reactive Intermediates. *Appl. Spectrosc.* **2011**, 65, 1087-1115.
17. Kukura, P.; Yoon, S.; Mathies, R.A. Femtosecond Stimulated Raman Spectroscopy. *Anal. Chem.* **2006**, 78, 5952-5959.
18. Umamathy, S.; Mallick, B.; Lakshmana, A. Mode dependent Dispersion in Raman Line Shapes: Observations and Implications from Ultrafast Raman Loss Spectroscopy. *J. Chem. Phys.* **2010**, 133, 024505
19. Kukura, P.; McCamant, D.W.; Mathies, R.A. Femtosecond Stimulated Raman Spectroscopy. *Ann. Rev. Phys. Chem.* **2007**, 58, 461-488.
20. Greetham, G.M.; Burgos, P.; Cao, Q.; Clark, I.P.; Codd, P.S.; Farrow, R.C.; George, M.W.; Kogimtzis, M.; Matousek, P.; Parker, A.W.; Pollard, M.R.; Robinson, D.A.; Xin, Z.J.; Towrie, M. ULTRA: A Unique Instrument for Time-Resolved Spectroscopy. *Appl. Spectrosc.* **2010**, 64, 1311-1319.
21. Shim, S.; Mathies, R.A. Development of a Tunable Femtosecond Stimulated Raman Apparatus and Its Application to  $\beta$ -Carotene. *J. Phys. Chem. B* **2008**, 112, 4826-4832
22. Weigel, A; Ernsting, N. Excited Stilbene: Intramolecular Vibrational Redistribution and Solvation Studied by Femtosecond Stimulated Raman Spectroscopy. *J. Phys. Chem. B* **2010**, 114, 7879-7893.
23. Jou, F-Y.; Freeman, G.R. Temperature and Isotope Effects on the Shape of the Optical Absorption Spectrum of Solvated Electrons. *J. Phys. Chem.* **1979**, 83, 2383-2387.
24. Razi Naqvi, K.; Li, H.; Melø, T.B., Webster, R.D. Spectroscopic Characterization of Neutral and Cation Radicals of  $\alpha$ -Tocopherol and Related Molecules: A Satisfactory Denouement. *J. Phys. Chem. A* **2010**, 114, 10795-10802.
25. Chen, X; Larsen, D.S.; Bradforth, S.E.; von Stokkum, I.H.M. Broadband Spectral Probing Revealing Ultrafast Photochemical Branching after Ultraviolet Excitation of the Aqueous Phenolate Anion. *J. Phys. Chem. A* **2011** 115, 3807-3819.

26. Buxton, G.V.; Greenstock, C.L.; Helman, W.P.; Ross, A.B. Critical Review of Rate Constants for Reactions of Hydrated Electrons, Hydrogen Atoms and Hydroxyl Radicals ( $\cdot\text{OH}/\text{O}^\cdot$ ) in Aqueous Solution. *J. Phys. Chem. Ref. Data* **1988**, 17, 513-886.
27. Steenken, S.; Neta, P. One-electron Redox Potentials of Phenols, Hydroxyphenols and Aminophenols and Related Compounds of Biological Interest. *J. Phys. Chem.* **1982**, 86, 3661-3667.
28. Edge, R.; Land, E.J.; McGarvey, D.; Mulroy, L.; Truscott, T.G. Relative One-electron Reduction Potentials of Carotenoid Radical Cations and the Interactions of Carotenoids with the Vitamin E Radical Cation. *J. Am. Chem. Soc.* **1998**, 120, 4087-4090.
29. Yao, W.W.; Peng, H.M.; Webster, R.D.; Gill, P.M.W. Variable Scan Rate Cyclic Voltammetry and Theoretical Studies on Tocopherol (Vitamin E) Model Compounds. *J. Phys. Chem. B* **2008**, 112, 6847-6855.
30. Huppert, D.; Kolodney, E.; Gutman, M.; Nachliel, E. Effect of Water Activity on the Rate of Proton Dissociation. *J. Am. Chem. Soc.* **1982**, 104, 6949-6953.
31. Pines, E.; Fleming, G.R. Proton Transfer in Mixed Organic Solvent Solutions - Correlation Between Rate, Equilibrium Constant, and the Proton Free Energy of Transfer. *J. Phys. Chem.* **1991**, 95, 10448-10457.
32. Man, Y.B.C.; Ammawath, W.; Mirghani, M.E.S. Determining  $\alpha$ -Tocopherol in Refined Bleached and Deodorized Palm Olein by Fourier Transform Infrared Spectroscopy. *Food Chem.* **2005**, 90, 323-327.
33. Bisby, R.H.; Ahmed, S. Transverse Distribution of  $\alpha$ -Tocopherol in Bilayer Membranes Studied by Fluorescence Quenching. *Free Radic. Biol. Med.* **1989**, 6, 231-239.
34. Dad, S.; Bisby, R.H.; Clark, I.P.; Parker, A.W. Singlet Oxygen Formation from Solutions of Vitamin E. *Free Radic. Res.* **2006**, 40, 333-338.
35. Max, J. J.; Chapados, C. Infrared Spectroscopy of Aqueous Carboxylic Acids: Comparison between Different Acids and their Salts. *J. Phys. Chem. A* **2004**, 108, 3324-3337.
36. Burton, G.W.; Ingold, K.U. Vitamin E - Application of the Principles of Physical Organic Chemistry to the Exploration of Its Structure and Function. *Accounts Chem. Res.* **1986**, 19, 194-201.
37. Barclay, L.R.C.; Vinqvist, M.R. Membrane Peroxidation - Inhibiting Effects of Water-soluble Antioxidants on Phospholipids of Different Charge Types. *Free Radic. Biol. Med.* **1994**, 16, 779-788.
38. Becke, A.D. Density-functional Exchange-energy Approximation with Correct Asymptotic Behavior. *Phys. Rev.* **1988**, A38, 3098-3100.

39. Perdew, J.P.; Wang Y. Accurate and Simple Analytical representation of the Electron-gas Correlation Energy. *Phys. Rev. B* **1992**, 45, 13244-13249.
40. Frisch, M. J.; Trucks, G. W.; Schlegel, H. B.; Scuseria, G. E.; Robb, M. A.; Cheeseman, J. R.; Scalmani, G.; Barone, V.; Mennucci, B.; Petersson, G. A.; Gaussian 09, Revision A.1, Gaussian, Inc., Wallingford, CT, 2009
41. Alberto M.E.; Russo, N.; Grand A.; Galano A. A Physicochemical Examination of the Free Radical Scavenging Activity of Trolox: Mechanism, Kinetics and Influence of the Environment. *Phys. Chem. Chem. Phys.* **2013**, 15, 4642-4650.
42. Nagaoka, S.; Kuranaka, A; Tsuboi, H.; Nagashima, U.; Mukai, K. Mechanism of Antioxidant Reaction of Vitamin E: Charge Transfer and Tunneling Effect in Proton-Transfer Reaction. *J. Phys. Chem.* **1992**, 96, 2754-2761.
43. Kohno, Y.; Fuji, M.; Matsuoka, C.; Hashimoto, H.; Ouchi, A.; Nagaoka, S.; Mukai, K. Notable Effects of the Metal Salts on the Formation and Decay Reactions of  $\alpha$ -Tocopheroxyl Radical in Acetonitrile Solution. The Complex Formation between  $\alpha$ -Tocopheroxyl and Metal Cations. *J. Phys. Chem. B* **2011**, 115, 9880-9888.



Ultrafast dynamics of tocopheroxyl radical formation following UV excitation.

Title: "Ultrafast Vibrational Spectroscopic Studies on the Photoionization of the  $\alpha$ -Tocopherol Analogue Trolox C"

Authors: Parker, Anthony; Bisby, Roger; Greetham, Gregory; Kukura, Philipp; Scherer, Kathrin; Towrie, Michael